



Dielectric and Ferroelectric Characterization of $\text{Na}(\text{Ta}_{1-x}\text{Nb}_x)\text{O}_3$ Solid Solution Ceramics

X.M. CHEN, Y.T. LU, D.Z. JIN & X.Q. LIU

Department of Materials and Engineering, Zhejiang University, Hangzhou 310027, China

Submitted April 5, 2004; Revised January 28, 2005; Accepted February 1, 2005

Abstract. Ceramics in the $\text{Na}(\text{Ta}_{1-x}\text{Nb}_x)\text{O}_3$ system were prepared by a solid state reaction approach, and their dielectric characteristics were evaluated together with the structures. The complete solid solution with orthorhombic structures was observed in the present system, and three supposed phase transitions at about 475, 580 and 650°C were observed by DTA. Only one dielectric anomaly was observed at high temperature for $x = 0.2$ and 0.4, and alternative dielectric anomaly (a diffused dielectric peak) was observed around 170 and 380°C for $x = 0.6$ and 0.8, respectively. The compositions of 0.6 and 0.8 are weakly ferroelectric and those of 0.2 and 0.4 are supposed to be antiferroelectric at room temperature.

Keywords: $\text{Na}(\text{Ta}_{1-x}\text{Nb}_x)\text{O}_3$, solid solution, dielectric properties, ceramics, sintering

1. Introduction

NaNbO_3 is known to exhibit typical antiferroelectric character in the vicinity of room temperature [1–5], and it has the ideal cubic perovskite structure with space group $\text{Pm}\bar{3}\text{m}$ above 641°C [2]. Below this temperature, several phases and the corresponding phase transitions at 575, 520, 480, 373 and –100°C have been reported [2, 4]. The curve of dielectric constant v.s. temperature indicates a sharp variation around 370°C, and no dielectric anomaly else is observed in the temperature range from 185 to 480°C [3].

On the other hand, the similar perovskite compound NaTaO_3 also has several phase transitions at 475, 580 and 650°C [6, 7]. Though the earlier work reported NaTaO_3 as a ferroelectric with Curie temperature about 475°C, the later detailed dielectric investigations by Iwasaki and Ikeda stated that there was no electric hysteresis loop or any anomaly in the $\varepsilon(T)$ curve observed either for the ceramic samples or single crystals [8]. Moreover, the dielectric anomalies were observed in the region of phase transitions, and the dielectric characteristics were very sensitive to the sintering conditions [9]. Though the structure in $\text{Na}(\text{Ta}_{1-x}\text{Nb}_x)\text{O}_3$ system was previously investigated by Iwasaki and Ikeda,

and two kinds of orthorhombic solid solutions were reported [8], the systematic investigation on dielectric characteristics in the solid solution system is lacking.

In the present work, ceramics in the NaNbO_3 – NaTaO_3 quasi-binary system are prepared by a solid state reaction approach, and their dielectric characteristics are investigated together with the structures.

2. Experimental Procedure

$\text{Na}(\text{Ta}_{1-x}\text{Nb}_x)\text{O}_3$ ceramics ($x = 0.2, 0.4, 0.6$ and 0.8) were prepared by a solid-state reaction process using reagent-grade NaHCO_3 (99.5%), Nb_2O_5 (99.99%), and Ta_2O_5 (99.99%) powders as the raw materials. The weighed raw materials were mixed by ball milling with zirconia media in de-ionized water for 24 h, and the mixtures were heated at 700 to 950°C in air for 3 h after drying. The $\text{Na}(\text{Ta}_{1-x}\text{Nb}_x)\text{O}_3$ powders calcined at their own optimum temperatures were used to yield ceramic samples by the following procedure. The calcined powders, with 6 wt% of PVA added, were pressed into disks measuring 12 mm in diameter and 2–6 mm high and then sintered at 1000 to 1525°C in air for 3 h.

The bulk density was evaluated by Archimedes method. Ground and thermal-etched surfaces of the sintered samples were observed by scanning electron microscopy (SEM, Hitachi S-570, Japan), and the crystal phases were determined by powder X-ray diffraction (XRD, Rigaku D/max 2550 pc, Japan) using Cu-K α radiation after crushing and grinding. The XRD data for Rietveld analysis was collected under the power of 40 kV \times 30 mA over the range of $2\theta = 10 - 130^\circ$ with a step size of $0.01^\circ/\text{s}$. DTA (SDT Q600 V5.0 Build 63, Universal V3.8 TA Instruments) analysis was carried out in the temperature range of 20 to 800°C to determine the phase transitions. The dielectric constant and dielectric loss were evaluated as the functions of temperature in the range of 50 to 600°C , using an LCR meter (Agilent 4284A), where the silver paste was used as the electrodes.

3. Result and Discussion

Figures 1 and 2 show the XRD patterns of various compositions calcined at optimal and inadequate temperatures respectively. All the compositions have orthorhombic perovskite structures, which can be further identified by the Rietveld analysis of the XRD data collected for dense ceramic powders with $x = 0.6$ and 0.8 . Minor amount of secondary phases are detected in the powders calcined at lower temperatures (see Fig. 2). Based on the above investigation, the optimum cal-

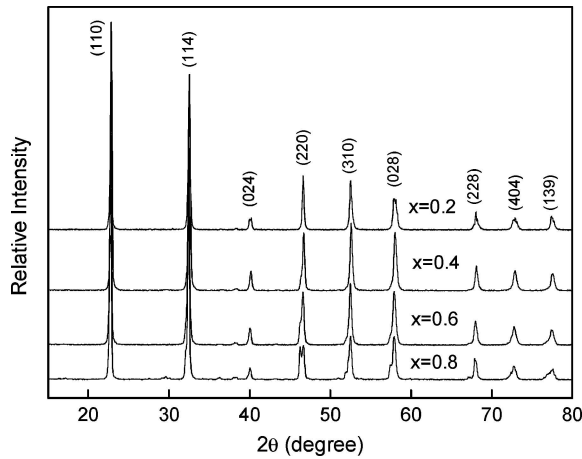


Fig. 1. XRD patterns of $\text{Na}(\text{Ta}_{1-x}\text{Nb}_x)\text{O}_3$ ceramic powders calcined at their optimal temperatures in air for 3 h: 950°C for $x = 0.2$; 750°C for $x = 0.4$ and 0.6 ; 700°C for $x = 0.8$.

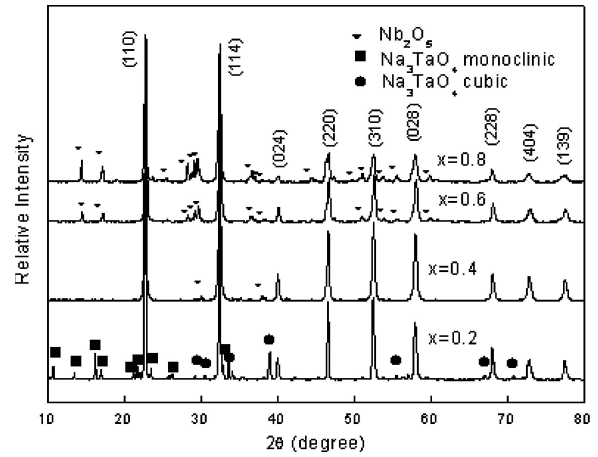


Fig. 2. XRD patterns of $\text{Na}(\text{Ta}_{1-x}\text{Nb}_x)\text{O}_3$ ceramic powders calcined at inadequate temperatures in air for 3 h: 850°C for $x = 0.2$; 700°C for $x = 0.4$ and 0.6 ; 650°C for $x = 0.8$.

cing temperatures are chosen as 950°C for $x = 0.2$, 750°C for $x = 0.4$ and 0.6 , and 700°C for $x = 0.8$. The lattice parameters of $\text{Na}(\text{Ta}_{1-x}\text{Nb}_x)\text{O}_3$ solid solution are listed in Table 1 as the functions of composition x .

Figure 3 and Table 2 show the Rietveld refinement results of the XRD data of ceramic powders. The R_p and R_{wp} values are determined to control the quality of the calculations. Small R_p and R_{wp} values ranging from 4–6% indicate high accuracy of the determination of phases by these refinement results. For all the compositions the orthorhombic structures (JCPDS Card No.73-0803) are identified with space group of Pbcm. The above results are in line with that reported by Iwasaki and Ikeda [8], where the orthorhombic structure has been identified in entire composition range of $\text{Na}(\text{Ta}, \text{Nb})\text{O}_3$.

Table 1. Variation of lattice parameters and room temperature dielectric characteristics of $\text{Na}(\text{Ta}_{1-x}\text{Nb}_x)\text{O}_3$ solid solution with composition x .

Composition	$x = 0.2$	$x = 0.4$	$x = 0.6$	$x = 0.8$	* $x = 1.0$
a (Å)	5.512	5.501	5.494	5.479	5.506
b (Å)	5.523	5.493	5.541	5.522	5.566
c (Å)	15.580	15.586	15.563	15.579	15.52
Cell volume (Å ³)	474.357	470.981	473.79	471.31	475.63
ϵ (at 100 kHz)	336.9	672.3	430.5	250.6	\
$\tan\delta$ (at 100 kHz)	0.0005	0.0014	0.0089	0.013	\
ϵ (at 1 MHz)	336.9	670.5	426.2	246.9	\
$\tan\delta$ (at 1 MHz)	0.0004	0.0015	0.0054	0.0095	\

*JCPDS Card No.73-0803.

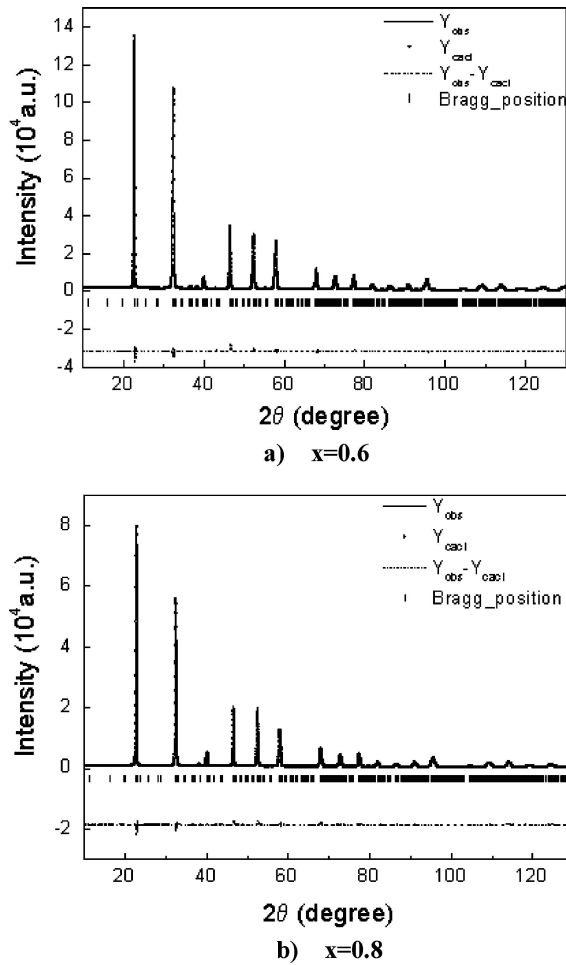


Fig. 3. Rietveld pattern of Na(Ta_{1-x}Nb_x)O₃ ceramics. Solid lines represent the observed intensity and dots represent the calculated. A difference (dashed dots) between the observed and the calculated are shown beneath. Vertical bars are the reflection position markers.

The densification characteristic of the present ceramics is shown in Fig. 4. Na(Ta_{1-x}Nb_x)O₃ ceramics with high relative density of 0.977T.D. (Theoretic density) is obtained by sintering around 1450°C for $x = 0.2$, and the highest relative density obtained for other compositions is just ranged from 0.93 to 0.95T.D., while the densification temperature is 1250, 1200 and 1050°C for $x = 0.4, 0.6$ and 0.8 , respectively. Figure 5 gives SEM micrographs of the present ceramics sintered at the above optimum temperatures for each composition. These micrographs indicate the relatively poor sinterability of the compositions for $x = 0.4, 0.6$ and 0.8 , where the sintering process is stopped at the

Table 2. Data for Rietveld refinement of Na(Ta_{1-x}Nb_x)O₃ ceramics with composition of 0.6 and 0.8.

Composition	$X = 0.6$	$X = 0.8$
Unit Cell (Space group Pbcm, 57)	$a = 5.49381(9)\text{Å}$ $b = 5.54146(8)\text{Å}$ $c = 15.5629(3)\text{Å}$ Volume = 473.79(1) Å ³	$a = 5.47863(9)\text{Å}$ $b = 5.52202(9)\text{Å}$ $c = 15.5790(3)\text{Å}$ Volume = 471.31(1) Å ³
R_p (profile)	0.0357	0.0472
R_{wp} (weighted profile)	0.0486	0.0625
R_B (Bragg)	0.0275	0.0390
R_F	0.0283	0.0470
Reduced χ^2	5.20	4.34
Total refined variables	38	40
Minimum 2θ	10	10
Maximum 2θ	130	130
No. of reflections	958	931
Profile function	Pseudo-Voigt ($\eta = 0.129$)	Pseudo-Voigt ($\eta = 0.179$)
Gaussian U, V, W	0.094, -0.085, 0.061	0.063, -0.066, 0.052
Asymmetry corrections (P1, P2)	0.002, 0.055	0.015, 0.055

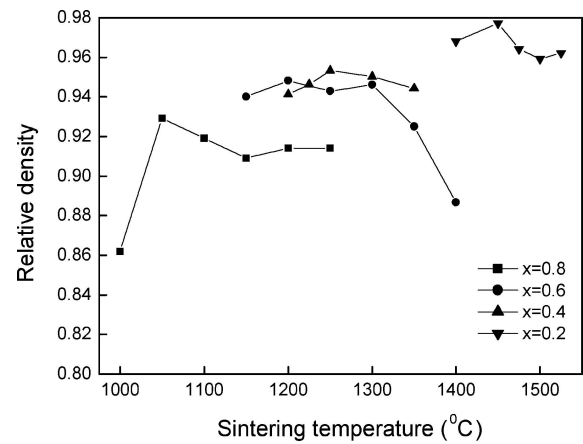


Fig. 4. Relative density of Na(Ta_{1-x}Nb_x)O₃ ceramics as functions of sintering temperature.

earlier stage and the final stage of sintering with microstructure development not completed. As we can see from Figs. 4 and 5, the sinterability decreases with increasing the content of niobium, and the composition of $x = 0.2$ indicates the best sinterability. SEM micrographs in Fig. 5 are all taken for the samples with the

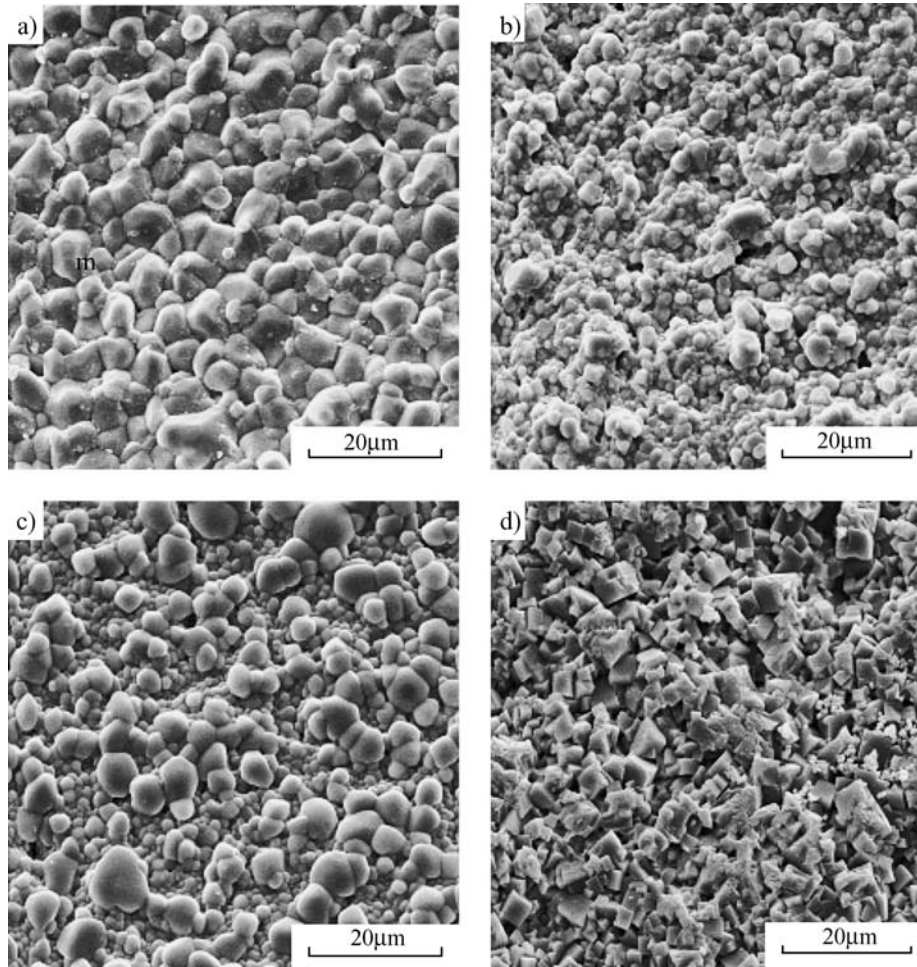


Fig. 5. SEM micrographs of $\text{Na}(\text{Ta}_{1-x}\text{Nb}_x)\text{O}_3$ dense ceramics: (a) $x = 0.2$; (b) $x = 0.4$; (c) $x = 0.6$; (d) $x = 0.8$.

highest density, and the samples sintered at either lower or higher temperatures all show lower density or even over sintering. So the uncompleted microstructure development in the compositions with higher x value is due to the poor sinterability of the solid solution itself but not due to the improper sintering regimes.

The DTA curves for the crushed powders of dense ceramics indicate that three phase transitions might occur at about 475, 580 and 650°C for all compositions investigated here (see Fig. 6). The peaks below 100°C in the DTA curves are concerning with the dehydration process. The above phase transition points well match those reported for the NaNbO_3 and NaTaO_3 end-members [2, 7].

The room temperature dielectric characteristics are also listed in Table 1. The dielectric constant ϵ

increases first and then decreases with increasing x both at 100 kHz and 1 MHz, while dielectric loss $\tan\delta$ increases all along. Figure 7 shows the temperature dependence of dielectric constant of the present ceramics. No dielectric peaks are observed at the temperatures where three phase transitions are supposed to occur by DTA data. However this contradiction does not indicate that the supposed three phase transitions do not exist. The similar phenomena have been reported in some previous work [6, 7, 9, 13–15]. It has been confirmed that NaTaO_3 experiences a series of phase transitions: orthorhombic (in rhombic orientation)/orthorhombic (in pseudocubic orientation)/tetragonal/cubic [6, 7, 13]. However, except Aleksandrowiz [9] who observed three endothermal peaks in his DTA experiment but only detected one

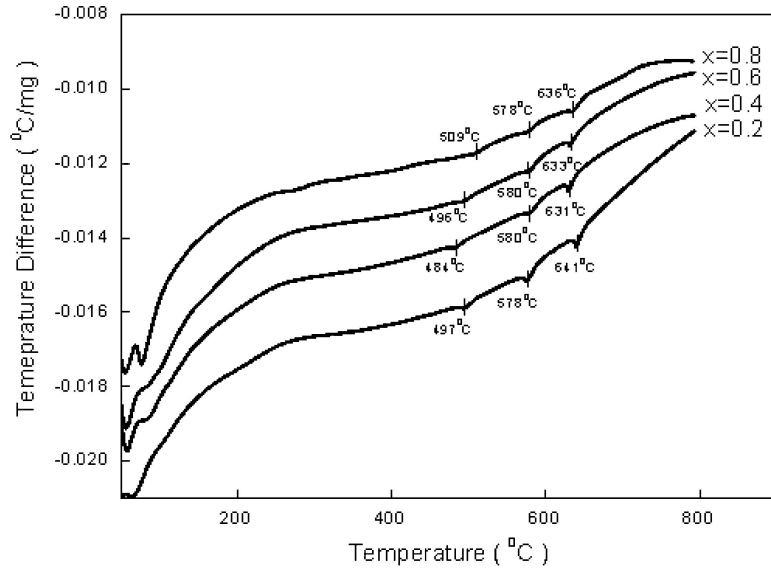


Fig. 6. DTA curves for crashed powders of Na(Ta_{1-x}Nb_x)O₃ dense ceramics.

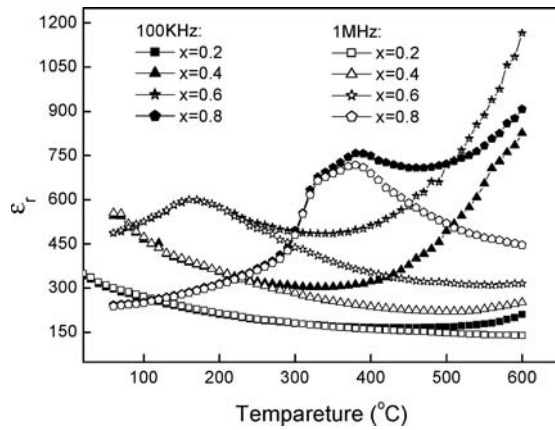


Fig. 7. Temperature dependence of dielectric constant of Na(Ta_{1-x}Nb_x)O₃ dense ceramics (60–600°C).

dielectric constant peak in the range of $-200\text{--}700^\circ\text{C}$, all others including Smolenski, Isupov [14, 15], Iwasaki and Ikeda [8] observed no dielectric constant peaks from helium temperature up to high temperature. Although the mechanism of this phenomenon is not clear, it does exist. The result in this paper is another evidence of this phenomenon. The possible conclusion is that these three phase transitions are not ferroelectric phase transition.

Though NaNbO₃ indicates a dielectric peak at 355°C [3], only one dielectric anomaly is observed

at high temperature for $x = 0.2$ and 0.4 , and alternative dielectric anomaly (a diffuse dielectric peak) is observed around 170 and 380°C for $x = 0.6$ and 0.8 , respectively. The high temperature dielectric anomaly is obvious at 100 kHz but almost absent at 1 MHz . This suggests that the dielectric anomaly observed at temperature above 400°C under frequency of 100 kHz is originated from the high temperature charge conductivity, while the diffuse dielectric peak at lower temperature is supposed to be the competitive effects of a second order phase transition and oxygen vacancies. The dielectric peak temperatures for $x = 0.6$ and $x = 0.8$ are close to those observed for $x = 0.56$ and 0.9 reported by Iwasaki and Ikeda [8], but the dielectric peaks are much diffuser than those reported by the previous authors. This difference might be due to the oxygen vacancies originated by the volatilization of sodium during sintering in the present work, and the oxygen vacancies contribute to the diffuse character of the dielectric anomaly [10–12].

The hysteresis loops of Na(Ta_{1-x}Nb_x)O₃ dense ceramics are shown in Fig. 8. It can be found that the remnant polarization increases with x and reaches the high of $6\ \mu\text{C}/\text{cm}^2$ when $x = 0.8$ although the remnant polarization of $x = 0.2$ and 0.4 are very poor. Iwasaki and Ikeda in their work have reported that the hysteresis loops of all the compositions are detected to be linear at room temperature and the loops indicating

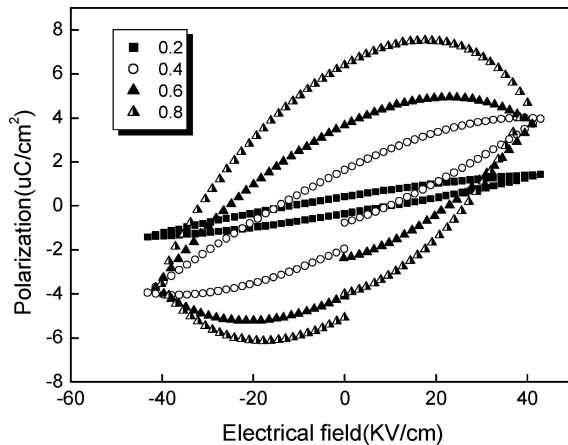


Fig. 8. Hysteresis loops of $\text{Na}(\text{Ta}_{1-x}\text{Nb}_x)\text{O}_3$ dense ceramics.

ferroelectricity are only detected below the temperature of dielectric peaks when $x < 0.55$. So the author concluded that a ferro-paraelectric transition takes place at the temperature (far below room temperature) where the dielectric peak occurs with the compositions of $x < 0.55$ and the other compositions are antiferroelectric at room temperature [8].

The results of our work indicate that the compositions of 0.6 and 0.8 are obviously ferroelectric though weak and the compositions of 0.2 and 0.4 should not be paraelectric given their orthorhombic crystal structures at temperature. However the compositions of 0.2 and 0.4 could be inferred to be antiferroelectric and the nearly linear loops (while not double loops) result from the inadequate maximum testing electric field due to the high electrical conductivity. The arch shapes of the loops are also caused by the high electrical conductivity of the solid solutions.

4. Conclusion

Dense ceramics with orthorhombic perovskite structures were obtained in the $\text{Na}(\text{Ta}_{1-x}\text{Nb}_x)\text{O}_3$ system

where the complete solid solution was observed. Three anomalies supposed to be caused by phase transition were observed at about 475, 580 and 650°C in the DTA curve. Only one dielectric anomaly was observed at high temperature for $x = 0.2$ and 0.4, and alternative dielectric anomaly (a diffused dielectric peak) was observed around 170 and 380°C for $x = 0.6$ and 0.8, respectively. The compositions of 0.6 and 0.8 are weakly ferroelectric and those of 0.2 and 0.4 are supposed to be antiferroelectric at room temperature.

Acknowledgment

This work was financially supported by National Science Foundation for Distinguished Yong Scholars under grant number 50025205 and Chinese National Key Project for Fundamental Researches under grant number 2002CB613302.

References

1. C.N.W. Darlington and H.D. Megaw, *Acta Cryst. B*, **29**, 2171 (1973).
2. C.N.W. Darlington, *Solid State Commun.*, **29**, 307 (1979).
3. G. Shirane, R. Newnham, and R. Pepinsky, *Phys. Rev.*, **96**(3), 581 (1954).
4. J. Chen and D. Feng, *Phys. Stat. Sol. A*, **109**, 427 (1988).
5. X.B. Wang, Z.X. Shen, Z.P. Hu, L. Qin, S.H. Tang, and M.H. Kuok, *J. Molecular Structure*, **385**, 1 (1996).
6. M. Ahtee and C.N.W. Darlington, *Acta Cryst. B*, **36**, 1007.
7. L.E. Cross, *Philo. Mag.*, **1**, 76 (1956).
8. H. Iwasaki and T. Ikeda, *J. Phys. Soc. Jpn.*, **18**(2) 157 (1963).
9. A. Aleksandrowicz and K. Kojcik, *Ferroelectrics*, **99**, 105 (1989).
10. B.S. Kang and S.K. Choi, *J. Apl. Phys.*, **94**, 1904 (2003).
11. Chen Ang and Zhi Yu, *Phys. Rev. B*, **62**, 228 (2000).
12. O. Bidault and P. Goux, *Phys. Rev. B*, **49**, 7868 (1994).
13. B.J. Kennedy, A. K. Prodjosantoso, *J. Phys. :Condens. Matter.*, **11**, 6319 (1999).
14. G.A. Smolenski and A.I. Arganowskaia, *DANSSSR.*, **97**, 237 (1954).
15. W.A. Isupov, *Izv. AN SSSR, I XXI.*, **3**, 402 (1957).